



GLOBAL JOURNAL OF RESEARCHES IN ENGINEERING: J
GENERAL ENGINEERING
Volume 16 Issue 4 Version 1.0 Year 2016
Type: Double Blind Peer Reviewed International Research Journal
Publisher: Global Journals Inc. (USA)
Online ISSN: 2249-4596 & Print ISSN:0975-5861

Effect of Step Depth and Angle in Kline-Fogleman (Kfm-2) Airfoil

By Fadi Mishriky & Paul Walsh

Ryerson University

Abstract- Recent years have witnessed extensive research efforts that aim at improving the aerodynamic performance of aircraft. While most of the efforts are drawn towards high-lift systems, simple and innovative designs like Gurney flaps, trapped vortex cavities and backward-facing steps can have a significant effect on enhancing the aerodynamic properties of airfoils. One of those simple ideas is the Kline-Fogleman modified airfoil (KFm-2), which is basically an airfoil with a backward-facing step on the upper surface located at midway the chord length. It is claimed that the step creates a low pressure recirculation region on the suction side of the airfoil that may enhance the lifting force. This study will numerically examine the ability of the KFm-2 design to enhance the lift and drag properties of a NACA 2412 at a high Reynolds number of 5.9×10^6 . The effect of the step depth and the step angle will be thoroughly examined.

Keywords: aerodynamics, stepped airfoil, backward-facing step, KFm-2 airfoil, CFD.

GJRE-J Classification: FOR Code: 090199



Strictly as per the compliance and regulations of :



Effect of Step Depth and Angle in Kline-Fogleman (Kfm-2) Airfoil

Fadi Mishriky ^α & Paul Walsh ^σ

Abstract- Recent years have witnessed extensive research efforts that aim at improving the aerodynamic performance of aircraft. While most of the efforts are drawn towards high-lift systems, simple and innovative designs like Gurney flaps, trapped vortex cavities and backward-facing steps can have a significant effect on enhancing the aerodynamic properties of airfoils. One of those simple ideas is the Kline-Fogleman modified airfoil (KFm-2), which is basically an airfoil with a backward-facing step on the upper surface located at midway the chord length. It is claimed that the step creates a low pressure recirculation region on the suction side of the airfoil that may enhance the lifting force. This study will numerically examine the ability of the KFm-2 design to enhance the lift and drag properties of a NACA 2412 at a high Reynolds number of 5.9×10^6 . The effect of the step depth and the step angle will be thoroughly examined.

Keywords: aerodynamics, stepped airfoil, backward-facing step, KFm-2 airfoil, CFD.

1. INTRODUCTION

The majority of aircraft today use high-lift systems to augment the wing's lifting capabilities at different flight regimes. The importance of these systems is emphasized during take-off and landing, when the wings are required to generate high lifting forces at minimal speeds. These hinged surfaces are employed in most commercial subsonic aircraft and controlled using heavy mechanical devices as pistons, screws, racks and pinions, etc. All these components add to the cost, mass and complexity of the aircraft. Wlezien et al. [1] stated that half the cost and complexity of an aircraft wing are due to the complexity of the high-lift system. In addition, the gaps between the surface and the wing significantly increase the drag forces and the noise. For these reasons, any less complex and innovative design should be examined.

One of the simplest potential solutions is a series of stepped airfoils designed by Kline and Fogleman (KFm-series). In the early 1960s, Richard Kline, who had the hobby of making paper airplanes, created a paper airplane design that could fly for long distances despite wind or turbulences.

He presented the paper airplane to his colleague Floyd Fogleman who saw that this model can

fly and resist stalling. The two men then filled a U.S. patent for a wedged-like airfoil that is hollow from below [2], and with further developments, they filled another patent in 1977 [3] for an airfoil with a backward-facing step on the pressure side, with one or more membranes pivotally hinged near the step. A new family of airfoils (KFm1 – KFm8) diverged from their patented designs, where backward-facing steps were installed on either side of the airfoil. The KFm airfoils gained popularity among the radio controlled airplane community from that time to date, with most users claiming better stability and enhanced aerodynamic performance. The step is supposed to intentionally separate the flow from the airfoil, and trap a recirculating vortex over its vicinity. This recirculating zone creates low pressure regimes on specific locations of the airfoil, and this may enhance the aircraft performance.

Inspired by the Kline-Fogleman airfoil designs, Fertis et al. [4] designed an airfoil with a backward-facing step on the upper surface of the airfoil, and they filled a U.S. patent for their design titled "Airfoil". Six years later, Fertis [5] published the experimental results of the design shown in his patent. The experimental tests were performed on NACA 23012 airfoil at a range of Reynolds numbers from $1e+5$ to $5.5e+5$, and a wide range of angle of attacks; from 2° to 38° . The results showed improved stall characteristics at all tested airspeeds, increased lift coefficients and increased functional lift-to-drag ratios over a range of angle of attacks. Fathi et al. [6] performed a number of experimental and numerical experiments at a Reynolds Number of $5e+5$ on 15 different configurations of a symmetric NACA 0012 airfoil with a backward-facing step on either sides. The results showed that a step on the lower side of the airfoil whose depth is half the thickness of the airfoil and extends to the trailing edge will increase the lift and the lift to drag ratio. For all other cases, especially when the step is on the upper surface, the drag coefficient significantly increases and leads to a drop in the lift to drag ratio. Cox et al. [7] compared the Rolf Girsberger (RG) -15 airfoil section with a KFm-2 step with the clean RG-15 airfoil at four low Reynolds Numbers between $2.8e+3$ and $1e+5$. Results revealed that at these Reynolds number, the addition of the KFm-2 step was found to have no useful aerodynamic benefits.

With most of the studies were performed at low Reynolds numbers, this paper will investigate the

Author α: Graduate Student at the Department of Aerospace Engineering, Ryerson University, Canada.
e-mail: fadi.mishriky@ryerson.ca

Author σ: Associate Professor at the Department of Aerospace Engineering, Ryerson University, Canada.
e-mail: paul.walsh@ryerson.ca

capabilities of the KFm-2 approach to enhance the aerodynamic performance of a NACA 2412 airfoil at a high Reynolds number of 5.9×10^6 . The KFm-2 airfoil employs a backward-facing step at the mid-chord location on the suction side of the airfoil as shown

Figure 1. This design is commonly encountered in cases of sliding morphing skins. In such designs, two rigid surfaces remain in contact and slide against each other during morphing. This interface introduces backward-facing steps on the wings' surface.

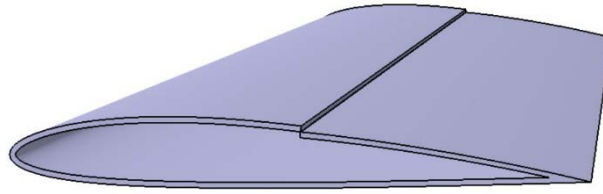


Figure 1: Kline-Fogleman (KFm-2) Airfoil with a backward-facing step mid-chord the upper surface of the wing.

The study will offer an in-depth numerical investigation on the effect of the step depth and the step angle on the aerodynamic properties of the airfoil. First, the numerical methodology and mesh independence study will be presented. The numerical testing will focus on variation of the lift coefficient c_l and the drag coefficient c_d with different step configurations. Finally, conclusion about the aerodynamics of the KFm-2 airfoil will be presented with general recommendations about the step depth and angle.

II. NUMERICAL MODELING AND BOUNDARY CONDITIONS

The commercial CFD code FLUENT is used in this study to simulate the flow using the finite volume method. An implicit density-based solver is used to solve the Navier-Stokes and the turbulence transport equations, where the convective and diffusive fluxes were calculated using a second-order Upwind scheme, and the gradients of scalar quantities were reconstructed using the Least-Squares cell-based method. The turbulence of the flow is modeled using the four equations Langtry-Menter transitional SST turbulence model [8, 9]. This model has been shown to accurately model the transition of the viscous boundary layer from laminar to turbulent which was observed to have an effect on the value of the lift and drag coefficients.

The airfoil used in the study is a standard NACA 2412 airfoil with a sharp trailing edge, a unity chord length and a computational domain that extends 32 chords in a C-grid topology. The air is treated as an ideal gas whose viscosity is calculated using the three equations Sutherland's formula.

The baseline parameters of the airfoil are from the NACA 2412 with a vertical step at the mid-chord with depth of 0.015 chord lengths. The NACA profile continues after the step, but scaled along the Y direction to intersect the step at its lower edge.

The mesh that discretizes the computational domain must compromise between computational accuracy and run time. To fulfill this challenging demand, a mesh independent study is performed using a family of three consecutively refined meshes with a constant refinement factor of $r = 2$. This means that for 2D meshes, the number of cells is quadrupled from each mesh to next refined one. The coarse, medium and fine meshes consist of 12,000, 48,000 and 192,000 cells, respectively. The Richardson's extrapolation method [10] is used to calculate the continuum value $\mathcal{F}_{h=0}$, where \mathcal{F} is an aerodynamic property that is evaluated on the coarse, medium and fine meshes to obtain \mathcal{F}_c , \mathcal{F}_m and \mathcal{F}_f respectively. In our case the lift coefficient c_l was used for this analysis.

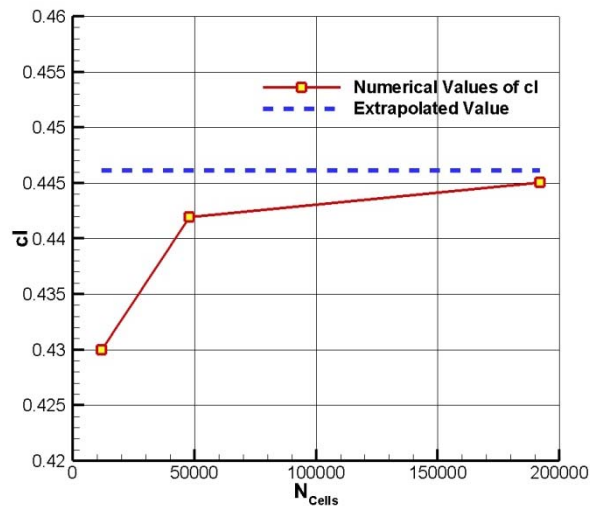


Figure 2: Convergence of the numerical value of c_l towards the extrapolated asymptotic value.

The continuum value $\mathcal{F}_{h=0}$ is calculated as follows:

$$\mathcal{F}_{h=0} \cong \mathcal{F}_f + \frac{\mathcal{F}_f - \mathcal{F}_m}{r^p - 1} \quad (1)$$

where r is the refinement ratio, and in our case it is constant at 2. While p is the observed order of accuracy of the solution and is calculated as:

$$p = \frac{\ln\left(\frac{\mathcal{F}_c - \mathcal{F}_m}{\mathcal{F}_m - \mathcal{F}_f}\right)}{\ln(r)} \quad (2)$$

This order of accuracy could be also calculated from the logarithmic slope of the errors of the three meshes ε_c , ε_m and ε_f . In this case, the error of \mathcal{F} in each mesh is calculated as:

$$\varepsilon_c = |\mathcal{F}_{h=0} - \mathcal{F}_c|, \quad \varepsilon_m = |\mathcal{F}_{h=0} - \mathcal{F}_m| \quad \text{and} \quad \varepsilon_f = |\mathcal{F}_{h=0} - \mathcal{F}_f| \quad (3)$$

Equations (1-3) were used to calculate the continuum value $\mathcal{F}_{h=0}$ of the lift coefficient. Figure 2 shows the values obtained from three meshes as well as the extrapolated continuum value. The value obtained from the fine mesh was 0.244% away from the asymptotic value $\mathcal{F}_{h=0}$.

This shows the adequacy of the fine mesh to capture the important physical features of the flow, and further refinements will only increase the computational time without notable improvement in the numerical accuracy. Thus, the fine mesh will be used in the next section to examine the effect of the step depth and angle on the aerodynamic performance of KFM-2 airfoil with a NACA 2412 profile.

III. RESULTS AND DISCUSSION

a) Effect of the step depth D_U

In this subsection, the effect of the step depth on the lift and drag coefficients of the airfoil will be tested. The flow is directed with an angle of attack of 2.5° over the NACA 2412 airfoil that has a vertical step. The location of the step is fixed at the mid chord length ($X/C = 0.5$), and the only variable will be the step depth. The testing starts with a step of depth $D_U/C = 0.0075$ and increase to $D_U/C = 0.025$ with an increment of $0.0025 C$ from one configuration to the other. Figure 3 shows the two extreme positions of the step depths representing $D_U/C = 0.0075$ and $D_U/C = 0.025$, where D_U is the step depth and C is the chord length.

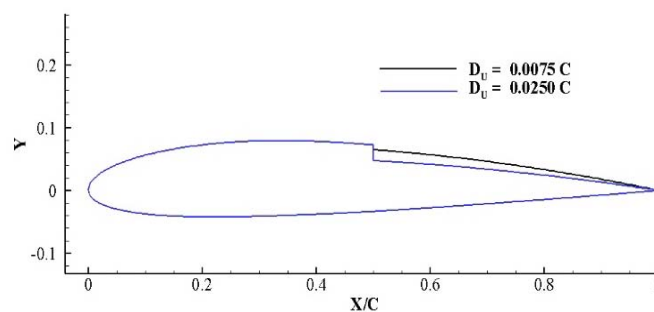


Figure 3: The two extreme depths of the step.

Eight configurations of different step depths were numerically simulated until convergence. The convergence criterion was judged by the complete stability of the lift, drag and moment coefficients.

As the depth gradually increased from $D_U/C = 0.0075$ to $D_U/C = 0.025$, the lift coefficient decreased by

about 20%, and the highest value of lift coefficient obtained (0.4812), is lower than the value obtained by the unchanged (clean) NACA 2412 which is equal to 0.5172. Figure 4 shows the inverse relation between the lift coefficient c_l and the step depth D_U .

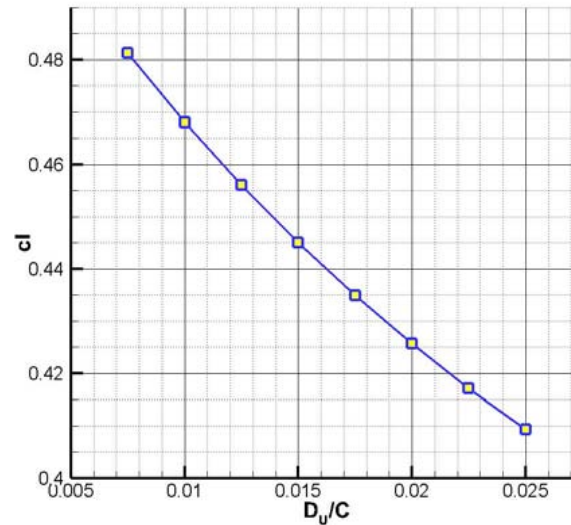


Figure 4: Effect of the step depth on the lift coefficient of the stepped NACA 2412 airfoil.

The steep slope of the curve in Figure 4 reflects the strong correlation between the step depth and lifting forces on the airfoil. To study the relation between the

lifting forces and the step depth, the pressure distribution over the eight configurations of step depths is shown in Figure 5.

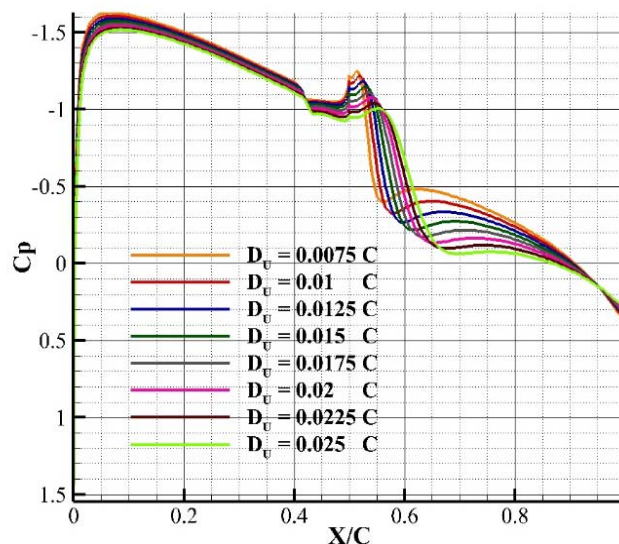


Figure 5: Pressure distribution over NACA 2412 airfoils with different step depths.

The step caused the airfoil thickness to locally decrease, which resulted in a deceleration of the flow as it traveled past the step, consequently increasing the value of the pressure after the step. As the step depth increased, the pressure increased on the suction side leading to an overall drop in the lift coefficient values.

It was also observed that the step depth affected the pressure distribution upstream the step

location, which increased as the step depth increased. Thus, from this analysis, it could be concluded that an increase in the step depth will cause the lifting forces to decrease.

Next, a similar analysis was performed to establish the relation between the drag coefficient and depth of the installed step. Results of this analysis are shown in Figure 6.

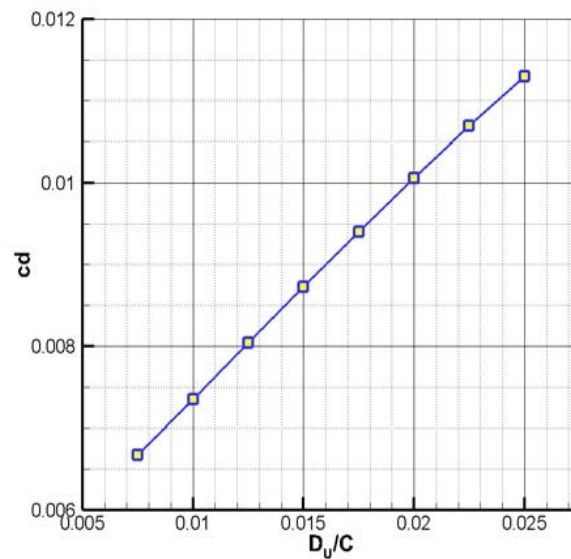


Figure 6: Effect of the step depth on the drag coefficient of the stepped NACA 2412 airfoil.

A linear-like relation is observed between the step depth D_u and the value of the drag coefficient of the airfoil. The lowest value of drag coefficient is still higher than the value obtained from the clean NACA 2412 at the same conditions. The drag coefficient value of a clean NACA 2412 is 0.00515, while the lowest drag coefficient in Figure 6 is observed at a step depth of $0.0075 C$, and is equal to 0.00668.

A nearly constant increment of $7e-4$ in the drag coefficient value is observed with each $0.0025 C$ increment in the step depth. This relation holds over the full testing range. To study this direct relation, the drag coefficient is decomposed to its two main components; the pressure drag coefficient and the viscous drag coefficient. Equation 4 provides the expression used to calculate each component.

$$c_d = c_p + c_f = \frac{1}{\rho v^2 A} \int_S (p - p_0)(\hat{n} \cdot \hat{i}) dA + \frac{1}{\rho v^2 A} \int \tau_w(\hat{t} \cdot \hat{i}) dA \quad (4)$$

Where c_p is the pressure drag coefficient, c_f is the friction drag coefficient or viscous drag coefficient, ρ is the fluid density, v is the reference velocity, A is the reference area, p is the pressure at the surface dA , p_0 is the reference pressure, \hat{n} is a unit vector normal to the surface dA , τ_w is the wall shear stresses at the surface dA and \hat{t} is a unit vector tangent to the surface dA .

The pressure drag coefficient is calculated as the surface integration of the pressure coefficient value acting normal to the airfoil surface, while the viscous drag component is the surface integration of the skin friction coefficient along the tangential direction of the airfoil surface. The results of this decomposition is shown in Figure 7.

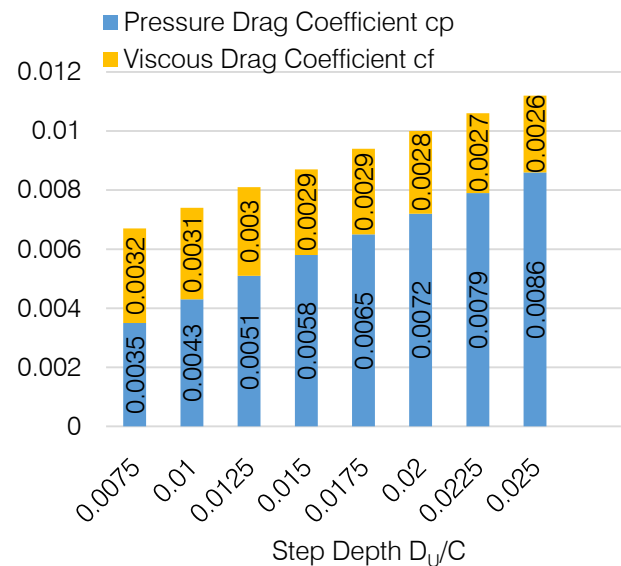


Figure 7: Decomposition of the Drag coefficient to pressure drag and viscous drag coefficients at different step depths.

The viscous drag coefficient experienced a small increase from one step depth to the other. On the other hand, the pressure drag coefficient is the dominant factor, and its contribution increased with the increase of the step depth. This is mainly due to the nature of the drag coefficient of stepped airfoils which is driven by the interaction of the low pressure region at the recirculation zone with the vertical wall of the step. With the increase of the step depth, the pressure experiences a slight increase, but the exposed area of the airfoil noticeably increases. This results in a constant increase in the pressure drag force acting on the step from one depth to the other. For that reason, the drag coefficient continuously increased as the step depth increased.

b) Effect of the step angle β

The previous subsection showed a strong correlation between the step depth and the values of the lift and drag coefficients. This subsection focuses on the effect of the KFM-2 step angle on the aerodynamic properties studied in the previous section.

Figure 8 shows five different configurations of the airfoil with the step angle rotated at different angles.

In all cases the step is fixed at $X=0.5 C$, with a step depth of $D_U=0.015 C$, while the step angle β changes from 45° to -45° , with the zero at the vertical position and positive angles are in the counter-wise direction.

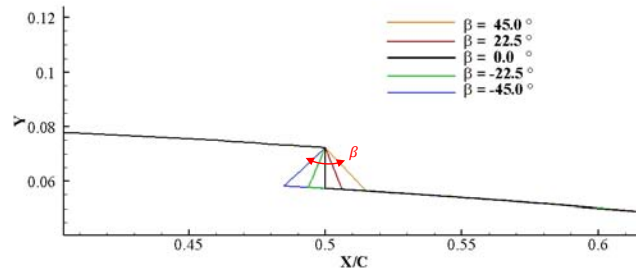


Figure 8: Different configurations of the NACA 2412 with different step angles.

The flow was set to an angle of attack of 2.5° in the simulations and the complete stability of the lift and drag coefficients marked the convergence of the

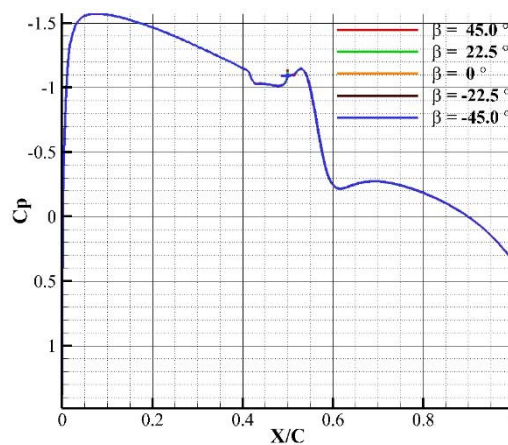
solution. Table 1 shows the lift and drag coefficients calculated at different step configurations.

Table 1: Values of the c_l , c_d and c_l/c_d at different step angles β .

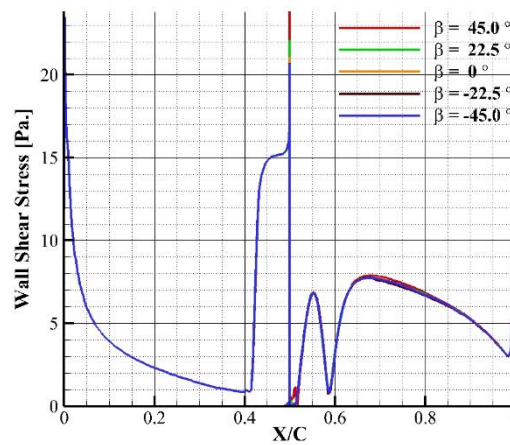
Step Angle	c_l	c_d	c_l/c_d
45.0°	0.44439	0.00878	50.6115
22.5°	0.44494	0.00873	50.9527
0°	0.44504	0.00873	50.9919
-22.5°	0.44503	0.00873	50.9779
-45.0°	0.44495	0.00873	50.9495

The five cases obtained nearly the same values for the lift and drag coefficients. This is confirmed by the identical values of the pressure distribution and the

shear wall stresses shown in Figure 9a and 9b respectively.



(a)



(b)

Figure 9: (a) Pressure distribution and (b) wall shear stresses of five different configurations with different step angles.

The identical curves justifies the equal results of the five configurations. A small difference is observed in the lift to drag ratio c_l/c_d in case of the angle $\beta=45^\circ$. This is due to the small displacement of the recirculation zone to the lower corner of the inclined step. In cases of step angles from $\beta=-45^\circ$ to 22.5° the recirculation zone started at $X/C = 0.513$, while in case of $\beta=45^\circ$, the bottom corner of the step started at $X/C = 0.517$, which is the location that marks the beginning of the recirculation zone. For that reason, the case with a step angle of $\beta=45^\circ$ obtained a slightly higher drag coefficient and lower lift coefficient when compared to the other cases. For cases with negative step angles, the additional space located at the cavity of the inclined step is filled with a cascade of minute low energy vortices that have negligible effect on the aerodynamics of the flow. Therefore, the effect of the step angle β ranging between 45 to -45° could be neglected in the aerodynamic analysis of backward-facing steps installed on the upper surfaces of airfoils.

IV. CONCLUSION

This study examined the aerodynamic performance of the KFM-2 airfoil with a NACA 2412 profile. Different variations of this design were achieved by changing the step depth and the step angle employed at the upper surface of the airfoil. The flow was simulated numerically at a Reynolds number of 5.9×10^6 , a Mach number of 0.16 and angle of attack of 2.5° . The study showed that employing a step on the upper surface of a NACA 2412 airfoil has degraded the aerodynamic performance in terms of the values of the lift and drag coefficients. The lift coefficient decreased as the step depth increased, while the drag coefficient followed a linear-like behavior that increased constantly as the step depth increased. Decomposition of the drag coefficient to its two main components revealed that for stepped airfoils, the pressure drag coefficient dominates

the calculation of the drag forces due to the interaction of the low pressure recirculation zone with the 'vertical' wall of the step. Changing the angle of the step from 45° to -45° did not have any effect on the drag and lift coefficients. Thus, employing a backward-facing step on the upper surface of a NACA 2412 at a high Reynolds number of 5.9×10^6 has degraded the aerodynamic performance when compared to the unchanged airfoil. However, decreasing the step depth diminishes these adverse effects.

REFERENCES RÉFÉRENCES REFERENCIAS

1. Wlezien, R.W., Homer, G.C., McGowan, A.R., Padula, S.L., Scott, M.A., Silcox, R.J. and Simpson, J.O. (1998). The Aircraft Morphing Program. *AIAA Paper* 98-1927.
2. Kline, R. L., & Fogleman, F. F. (1972). U.S. Patent No. 3706430. Washington, DC: U.S. Patent and Trademark Office.
3. Kline, R. L., & Fogleman, F. F. (1977). U.S. Patent No. 4,046,338. Washington, DC: U.S. Patent and Trademark Office.
4. Fertis, D. G., & Smith, L. L. (1986). *U.S. Patent No. 4,606,519*. Washington, DC: U.S. Patent and Trademark Office.
5. Fertis, D. G. (1994). New airfoil-design concept with improved aerodynamic characteristics. *Journal of Aerospace Engineering*, 7(3), 328-339.
6. Finaish, F., & Witherspoon, S. (1998). Aerodynamic performance of an airfoil with step-induced vortex for lift augmentation. *Journal of Aerospace Engineering*, 11(1), 9-16.
7. Cox, M. J., Avakian, V., & Huynh, B. P. (2014, December). Performance of a Stepped Airfoil at Low Reynolds Numbers. In *Proceedings of the 19th Australasian Fluid Mechanics Conference*, RMIT University, Melbourne, Australia.

8. Langtry, R. B., & Menter, F. R. (2009). Correlation-based transition modeling for unstructured parallelized computational fluid dynamics codes. *AIAA journal*, 47(12), 2894-2906.
9. Menter, F. R., Langtry, R., & Völker, S. (2006). Transition modelling for general purpose CFD codes. *Flow, Turbulence and Combustion*, 77(1-4), 277-303.
10. Shyy, W., Garbey, M., Appukuttan, A., & Wu, J. (2002). Evaluation of Richardson extrapolation in computational fluid dynamics. *Numerical Heat Transfer: Part B: Fundamentals*, 41(2), 139-164.